Y. S. Zhang, H. G. Ding
(Department of Precision Instruments Tsinghua University, Beijing, 100084, P. R. China)

INVESTIGATION OF THE SYSTEM CONFIGURATION FOR MICRO OPTIC GYROS

The re-entrant system configuration of optic gyro was investigated at Tsinghua University for developing the micro optic gyro (MOG). In the system, the bi-directional light beams are circulating in the Sagnac sensing ring (SSR) for many round trips. The feasibility of the proposed system was proved by the test results on the fiber analog experimental setup.

Introduction. Since 1980, the micro-nano technology has been applied extensively in the field of micro sensors. One of the outstanding examples is the micro integrated vibration gyro on silicon substrate (MSG). The MSG is developed as a micro electro-mechanic system (MEMS) with very low price.

Obviously, optic gyros are facing the challenge in the market of navigation products. Since 1983, people tried to use the integrated optic (IO) ring cavity to replace the mirror system resonator in the conventional ring laser gyro. Northrop company in USA had developed the first prototype of micro optic gyro (MOG), in which a passive IO resonator was used. Unfortunately, the MOG program of Northrop company stopped on the half way and the first MOG had not been developed as a gyro product.

In 1997, the LETI of CEA in France has developed the solid-state optic gyro (SSOG), in which the eight-turn optic waveguide coil with the diameter of 30 mm and the length of 800 mm was used for replacing the sensing coil in the conventional interferometer fiber optic gyro (IFOG). The advanced IO technology on silicon substrate ($IOS2$) insured the quality of the sensing coil with the optic loss coefficient < 0.025 dB/cm. By using $IOS2$ technology, LETI developed many other devices successfully. But due to the low accuracy caused by the short sensing coil, the SSOG did not find application in navigation system.

Since 1995 the authors at Tsinghua University started to investigate the MOG with IO sensing ring or coil. The goal of the investigation is to develop the MOG with the performance better than the existing miniature

[1] The paper is published without any redaction.

optic gyros, such as the GG1308 of Honeywell company and the $\mu FORS$ of LITEF company. The required performance of the MOG to be developed is shown in Table 1

Table 1

Characteristics of the MOG to be developed

Range of measurement	500 deg/s
Resolution	0.1–1 deg/h
Bias stability	1–10 deg/h
Scale factor errors	100–500 ppm
Bandwidth	200 Hz

For investigating the proposed re-entrant interferometer MOG, a fiber anlogue experimental setup was developed at Tsinghua University, in which the elements of conventional IFOG are used, such as the high quality superluminescent diode (SLD), the multi-functional IO phase modulator chip (MIOC), and the all digital closed loop electronics (ADCL).

Proposed interferometer system configuration. The setup of the proposed MOG system and the main elements are shown in Fig. 1 and Table 2, respectively. In the system configuration, an input / output coupler A is designed for transmitting the bi-directional light beams into the Sagnac sensing ring (SSR) and then back to the MIOC.

In case of open loop operation, the optical intensity detected by the photodiode (PD) is the sum of the optical responses of light beams with different number of round-trips. The resolution of the MOG system can be determined as

$$\Delta\Omega_{\min} = \frac{\lambda c}{2\pi MLD} \frac{\sqrt{4h\nu \cdot T(\phi_s)}}{\sqrt{\eta_D t_i} \cdot S(\phi_s)\sqrt{P_{in}}},$$

where M is the number of round-trips circulated; λ, c are the wavelength and the light speed, respectively; L, D are the length and the diameter of SSR, respectively;h is Plank's constant; ν is the light angular frequency;

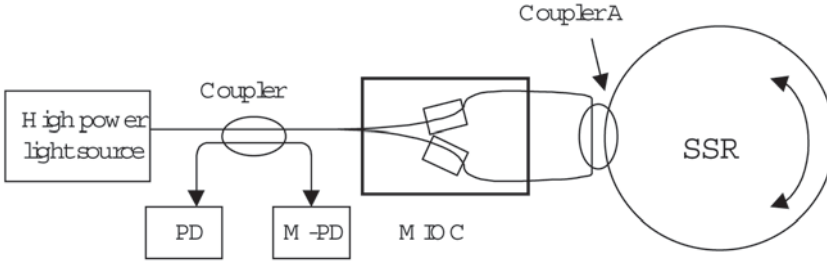

Fig. 1. The system configuration of re-entrant interferometer optic gyro

Parameters of the system in comparison with IFOG

Element	Conventional IFOG	The setup
1.3μm SLD	Output power $> 200\mu$W	Output power $> 600\mu$W
SSR (or coil)	Length 500–1000 m	Length < 200 m
Beam splitter (50 : 50)	Extinction ratio > 20 dB The same Insertion loss < 0.2 dB	
MIOC Splitting ratio (49.6/50.4)	Insertion loss < 3 dB Extinction ratio > 40 dB Bandwidth 500 MHz	The same
Coupler A (90 : 10)	No need	Extinction ratio > 20 dB Insertion loss < 0.2 dB

η_D, P_{in} are the efficiency of PD and the power of the SLD, respectively; $T(\phi_s) = 4p{+}2q\sum_{m=1}^{M}\eta^{2m}\left[1+\cos(2m\phi_s)\right]$ is the light transmission coefficient inside the SSR; $S(\phi_s) = \left|\dfrac{dT(\phi_s)}{d(\phi_s)}\right|$ is the scale factor.

In the system configuration with passive SSR, the resolution of the system depends significantly on the power coupling ratio of coupler A. In order to ensure the maximum SF and the best resolution, the coupling ratio (90 : 10) should be selected.

Development of the super luminescent diode. For the proposed MOG system, a superluminescent diode (SLD) with the output power of 0.6–1.0 mW is required. Suppose the coupling efficiency between the SLD chip and the PM fiber pigtail is around 30 %, the output power of the SLD chip should be higher than 3 mW at the injection current of 100 mA and the temperature of 20°C.

To realize the SLD, low optical loss, high internal quantum efficiency, and high gain are the three key features for the epitaxial layers. The epitaxial structures for the emission wavelength at 1300 nm were grown by metal organic chemical vapor deposition (MOCVD) on S doped n-type (100)-eriented InP substrate. All the layers were lattice-matched to the InP wafer except for the QWs, which were grown with a compressive strain.

We have designed and fabricated three epitaxial layers with different structures, doping profile in p-cladding layers, and the number of QWs. Finally, we selected the structure, which contains eight QWs. In the structure, a graded-refractive-index separate confinement heterostructure (GRIN-SCH) is used for realizing four energy steps from 1.1 to 1.3 eV with

thicknesses of 80, 60, 40, and 20 nm, respectively. Within each step the energy is further linearly graded. The etch stop layer in the p-cap layer in 20 nm thick 150 nm above the SCH region. The p-InP cap layer is linearly graded doped from a concentration of $2 \times 10^{17}\,\mathrm{cm}^{-3}$ to $9 \times 10^{17}\,\mathrm{cm}^{-3}$ within 500 nm. The characteristics of the developed SLD are shown in Table 3

Table 3

Characteristics of the developed SLD

Parameter	Measured result
Internal quantum efficiency	$\eta_i = 93\%$
Internal optical absorption at threshold	$\alpha_i = 11\,\mathrm{cm}^{-1}$
Characteristic temperature (20−60°C)	$T_0 = 58.2\,\mathrm{K}$

In order to suppress the spectrum modulation, facet reflectance must be minimized. We have designed the SLD, which is composed of a J-shape waveguide with 2-μm ridge and a tapered rear absorption region. The curvature of the waveguide suppresses the Fabre-Perot (FP) mode so that the device has only a single-pass amplified spontaneous emission (ASE). The tapered part is used to enhance the ASE, which has an open angle of 5°. The whole cavity is tilted against the facet with an angle of 8°.

The structure is etched to a depth of 1.4μm. The side wall of the ridge and the surface of the absorption area are coated with 200 nm SiO_2 deposited by electron-cyclotron plasma-enhanced chemical vaper deposition (ECP-PECVD). The ridge part of the SLD is 1.4 mm long and the whole absorption section is 1.5 mm long. After cleavage, the front facet of the SLD is coated with one layer of SiN_X as the anti-reflection film deposited by ECP-PECVD.

Characteristics of the developed SLD chip are shown in Table 4.

Table 4

Characteristics of the developed SLD chip

Parameter	Test result
Output power at 400 mA and 20°C	25 mW
Full-width at half-maximum (FWHM)	26–28 nm
Fluctuation on the spectrum (Ripple)	0.2 dB

Experimental investigation. The setup in closed loop operation is different from the conventional IFOG. In order to avoid the overlap of the signals with different numbers of round-trips, a pulsed phase modulation

approach is used for separating and selecting the needed signal. The pulse width is selected to be equel to the group transition time τ through the SSR and the modulation frequency is selected to be $2/(N+1)$ of the SSR eigen frequency.

In the passive SSR, the CW and CCW light beams can only propagate 2–4 round trips, after that, they will be shadowed by the shot noise of the PD and can not be detected. Therefore, in the case of passive SSR, $N = 4$ is chosen. In the setup, the length of SSR is 200 m, and the pulsed phase modulation frequency is 200 kHz. The time interval between the two pulses is $N\tau$.

The phase biasing is realized by the MIOC. The peak voltage is designed to be equel to the half-wave voltage of MIOC for alternately realizing the optimal phase bias of $\pm\pi/2$.

In order to improve the Signal-Noise-Ratio (SNR), the pulsed phase modulation has been modified by using a pair of positive and negative modulation pulses with the same amplitude and width τ. In this case, a subtrator should be used in the ADCL for processing the paired signals.

As mentioned before, the small couplng ratio α will lead to waste the SLD output light power and cause the saturation of the pre-amplifier circuits after the PD due to the increment of the DC component. In this case, the Sagnac effect signals of light beams after 3–4 round trips will be difficult to be detected. Therefore, in the setup the pre-amplifier has been re-designed by adding a special cascade for completely cutting off the DC component before amplification.

In order to investigate the performance of the proposed system for MOG, a specially designed ADCL electronics has been developed, in which the above mentioned phase modulation approach is realized. The setup with the ADCL electronics provides the digital readout as a gyro.

In the drift rate test, the samples of the Sagnac phase shift signals after 2 round-trips are selected with the sampling frequency equal to the modulation frequency (200 kHz). In every eight sampling periods, one digital data processing cycle has to be completed for providing the digital readout data. The data processing cycle includes signal sampling, demodulation, integration and digital ramp signal generation.

The random drift rate of the setup was tested with the integration time of 10 s and the sampling length of 0.5 h. The standard deviation of the drift rate is 1.25 deg/h.

The same drift rate test has been carried out on the setup, but with the additional monitoring PD (M-PD in Fig. 1). As shown by the test results, with the same integration time and the same sampling length, the standard deviation of the drift rate has been reduced to 0.75 deg/h.

The test results proved the effectiveness of the M-PD in the improvement of accuracy.

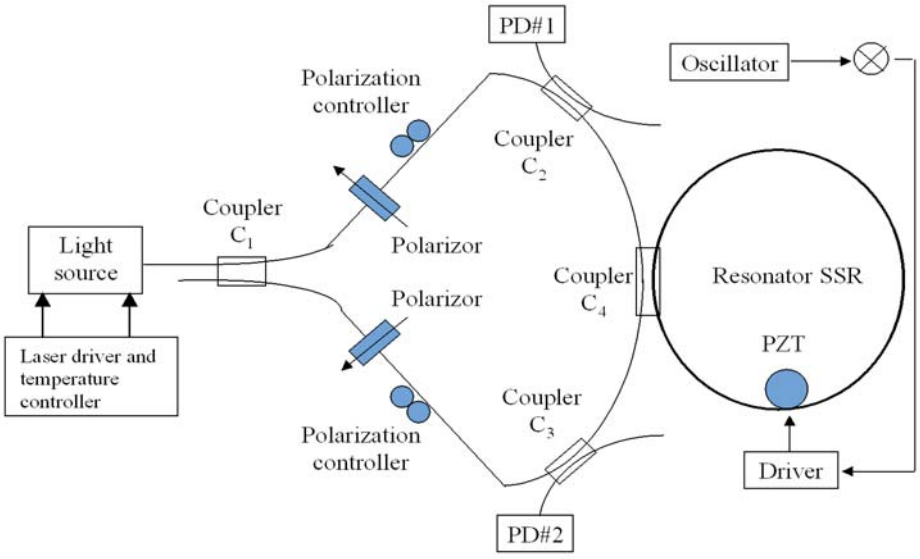

Fig. 2. The fiber analogue resonator system configuration for MOG

Comparison with the resonator system configuration. In 1997, the authors have developed a fiber analogue experimental setup of the resonator system configuration for MOG, in which a short PM fiber optical SSR was used. The system configuration and its elements are shown in Fig. 2 and Table 5, respectively.

Table 5

Elements used in the setup

Element	Parameters
SSR	Length 10 m
PM couplers C_1, C_2, C_3 Coupling ratio 50:50	Extinction ratio > 20dB, Insertion loss < 0.2dB
PM coupler C_4 Coupling ratio 10:90	Extinction ratio > 20dB, Insertion loss < 0.2dB
Polarizor	Extinction ratio > 20dB
Polarization controller	Extinction ratio > 40dB

Considering only the coupling ratio and losses in SSR and C_4, the calculated finesse of the resonator is around 50.

In the resonator MOG, the SSR and the light source are two key elements, which should be developed carefully. The best approach is to

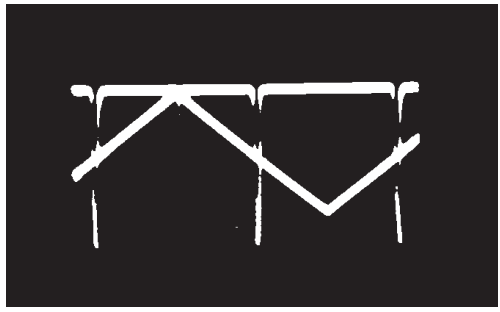

Fig. 3. The resonant waveform in the fiber analogue setup

combine the SSR and the light together in one element by doping the optical waveguide to form an active SSR.

In 1997, the task to develop an active SSR was difficult to be completed, we had to use separately the passive SSR and the light source with extremely narrow linewidth.

Firstly, a high power 25 mW Nd-YAG laser was used in the setup and the measured finesse of the passive SSR is around 35–40. According to the measured finesse, the linewidth of the Nd-YAG laser has been calculated as around 240 kHz. This value coincides with the real linewidth of the Nd-YAG laser.

Considering that the Nd-YAG laser is not suitable to be used in the MOG product, we have developed a fiber Bragg grating FBG-LD with narrow linewidth. As shown by the measured result, the linewidth is around 1.5 MHz.

The FBG-LD was used in the setup for replacing the Nd-YAG laser. As shown in the resonant waveform in the SSR (Fig. 3), the actual finesse of SSR is about 20–25. Obviously, the linewidth of the light source reduced the finesse of SSR significantly.

In comparison with the resonant system configuration, the proposed interferometer system configuration is easier to be realized on the base of the matured elements, used in IFOG, including the light source SLD, the MIOC, and the closed loop control electronics.

For developing the MOG with higher accuracy, in both system configurations, the active waveguide SSR is necessary to be used, because in the proposed interferometer system configuration, the number of round trips of light beams in the passive SSR is < 5.

Conclusions. 1. In the near future, the proposed re-entrant interferometer system configuration with passive SSR is feasible for the development of the MOG with moderate accuracy. This kind of MOG is realistic to be developed, because the elements of the MOG are compatible with those used in IFOG, which are matured industrial products.

2. For developing the MOG as a navigation grade gyro, the active SSR is necessary to be developed in either the interferometer or the resonator system configuration.

REFERENCES

1. A. W. Lawrence. The Micro-Optic Gyro, Symposium Gyro Technology, Stuttgart, Germany (1983).
2. A. Yu, A. S. Siddiqui. Novel Fiber Optic Gyroscope with a Configuration Combining Sagnac Interferometer with Fiber Ring Resonator, Electronics Lett. Vol. 28, No. 19, pp. 1778–1779 (1992).
3. P. Motteir. Integrated Optics at the LETI, International Journal of Optoelectronics, 9 (2), pp. 125–134 (1994).
4. Y. S. Zhang, B. Zhang, X. Y. Ma. Techniques for Developing a Miniature Resonant Optic Rotation Sensor, Proceedings of the 52nd Annual Meeting, June 19–21, Cambridge, MA, pp. 719–723 (1996).
5. H. G. Ding, Y. S. Zhang et al. Key Technologies of Micro Inertial Measurement Unit, Chinese Journal of Scientific Instrument, Vol. 17, No. 1, pp. 31–35 (1996).
6. P. Motteir, P. Pouteau. Solid State Optical Gyrometer Integrated on Silicon, Electronic Letters, Vol., 33, No. 23, Nov., pp. 1975–1977 (1997).
7. Y. S. Zhang, X. Y. Ma, B. Zhang, Q. A. Tang, Z. W. Pan, Q. Tian, A. Y. Zhang, M. Li, M. Zhang. Investigation of the Elements for Integrated Optic Gyro, The Second International Symposium on Inertial Technology (BISIT), October, Beijing, pp. 173–178 (1998).
8. L. Z. Wu, Y. S. Zhang, H. Schweizer. The Feasibility of Compact Gyroscope Realized by Semiconductor Ring Laser, Symposium Gyro Technology, Stuttgart, Germany (1999).
9. C. Ford, R. Ramberg, K. Johnsen, W. Berglund, B. Ellerbusch, R. Schermer, A. Gopinath. Cavity Element for Resonant Micro Optical Gyroscope, IEEE AES Systems Magazine, December, pp. 33–36 (2000).
10. Y. Zhang, F. Gao, X. Wu, W. Tian, Z. Hu, Q. Tian, Z. Pan, Q. Tang. Investigation of the Re-entrant Integrated Optical Rotation Sensor, Symposium Gyro Technology, Stuttgart, Germany (2000).
11. Y. Zhang, W. Tian, L. Fu, H. Schweizer. Experimental Research on a Novel Interferometric Fiber Optical Gyro with Light Beams Circulating in the Sagnac Sensing Ring, Symposium Gyro Technology, Stuttgart, Germany (2002).
12. L. Fu, H. Schweizer, Y. Zhang, L. Li, A. M. Baechle, S. Jochum, G. C. Bernatz, S. Hansmann. Design and Realization of High-Power Ripple-Free Super luminescent Diodes at 1300 nm, IEEE J. of Quantum Electronics, Vol. 40, No. 9, pp. 1270–1274 (2004).

Статья поступила в редакцию 8.07.2005

Хенгао Дин защитил кандидатскую диссертацию в 1961 г. в Ленинградском институте точной механики и оптики. Профессор Пекинского университета Цингуан, Президент Китайского общества технологий инерциальной навигации.

Henggao Ding received the Ph. D. degree from the Leningrad Institute of Fine Mechanics & Optics, in 1961. He is Professor of the Tsinghua University (China) and President of Chinese Society of Inertial Technology.

Яньшен Чжан защитил кандидатскую диссертацию в 1957 г. в МВТУ им. Н.Э. Баумана. С 1983 г. читает лекции в университете в Калгари, Стенфордском университете, в Штутгартском университете, в Институте наведения летательных аппаратов DFVLR и в Мюнхенском военном университете. Вице-президент Китайского общества технологий инерциальной навигации. Член Международной геодезической ассоциации, Американского оптического общества, Международного инженерного общества IEEE в области лазерной и оптико-электронной техники. Специализируется в области систем навигации, лазерных гироскопов и фотонных интегрирующих систем.

Yanshen Zhang received the Ph. D. (Eng.) degree from the Bauman Moscow Higher Technical School in 1957. In 1958, he founded the "Division for Navigation & Control" at Tsinghua University. In 1976, the first electrostatic gyro (ESG) and platform in China were developed under his leadership, and he was the Chief Designer of the ESG State Research Program during 1980–1990. Since 1983, he visited the University of Calgary, Stanford University, the University of Stuttgart, the Institute for Flight Guidance DFVLR, and the Munich Armed Forces University. His current interests are navigation systems, optical gyros and photonic integrated devices. He is an associate of the International Association of Geodesy, a member of the Optical Society of America (OSA) and a member of the IEEE Lasers and Electro-Optics Society (LEOS). His current interests are navigation systems, optical gyros and photonic integrated devices. the Vice President of the Chinese Society of Inertial Technology.
